molecular pharmaceutics

ARTICLE

pubs.acs.org/molecularpharmaceutics

A 3-in-1 Polymeric Micelle Nanocontainer for Poorly Water-Soluble Drugs

Ho-Chul Shin,[†] Adam W. G. Alani,[‡] Hyunah Cho,[†] Younsoo Bae,[§] Jill M. Kolesar,[∥] and Glen S. Kwon*[,†]

[†]Pharmaceutical Sciences Division, School of Pharmacy, University of Wisconsin−Madison, 777 Highland Avenue, Madison, Wisconsin 53705-2222, United States

[‡]Pharmaceutical Sciences Division, College of Pharmacy, Oregon State University, 1601 SW Jefferson Street, Corvallis, Oregon 97331, United States

[§]Pharmaceutical Sciences Division, College of Pharmacy, University of Kentucky, 789 South Limestone Street, Lexington, Kentucky 40536, United States

[∥]Pharmacy Practice Division, School of Pharmacy, University of Wisconsin−Madison, 600 Highland Avenue, Madison, Wisconsin 53792

Supporting Information

ABSTRACT: Poly(ethylene glycol)-*block*-poly(D,L-lactic acid) (PEG-*b*-PLA) micelles have a proven capacity for drug solubilization and have entered phase III clinical trials as a substitute for Cremophor EL in the delivery of paclitaxel in cancer therapy. PEG-*b*-PLA is less toxic than Cremophor EL, enabling a doubling of paclitaxel dose in clinical trials. We show that PEG-*b*-PLA micelles act as a 3-in-1 nanocontainer for paclitaxel, 17-allylamino-17-demethoxygeldanamycin (17-AAG), and rapamycin for multiple drug solubilization. 3-in-1 PEG-*b*-PLA micelles were ca. 40 nm in diameter; dissolved paclitaxel, 17-AAG, and rapamycin in water at 9.0 mg/mL; and were stable for 24 h at 25 °C. The half-life for *in vitro* drug release ($t_{1/2}$) for 3-in-1 PEG-*b*-PLA micelles was 1−15 h under sink conditions and increased in the order of 17-AAG, paclitaxel, and rapamycin. The $t_{1/2}$ values correlated with log $P_{o/w}$ values, implicating a diffusion-controlled mechanism for drug release. The IC_{50} value of 3-in-1 PEG-*b*-PLA micelles for MCF-7 and 4T1 breast cancer cell lines was 114 ± 10 and 25 ± 1 nM, respectively; combination index (CI) analysis showed that 3-in-1 PEG-*b*-PLA micelles exert strong synergy in MCF-7 and 4T1 breast cancer cell lines. Notably, concurrent intravenous (iv) injection of paclitaxel, 17-AAG, and rapamycin using 3-in-1 PEG-*b*-PLA micelles was well-tolerated by FVB albino mice. Collectively, these results suggest that PEG-*b*-PLA micelles carrying paclitaxel, 17-AAG, and rapamycin will provide a simple yet safe and efficacious 3-in-1 nanomedicine for cancer therapy.

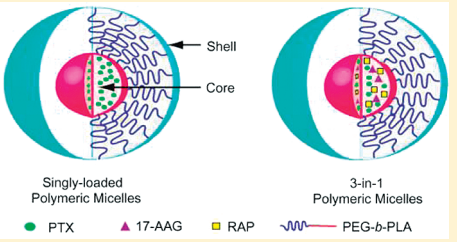

KEYWORDS: drug combination, heat shock protein 90, mammalian target of rapamycin, multiple drug solubilization, polymeric micelles, tanespimycin

1. INTRODUCTION

Novel combinations of molecularly targeted agents with chemotherapy, e.g. paclitaxel (PTX), have gained increasing attention in research that aims to overcome drug resistance and tumor heterogeneity for highly effective cancer regimens, noting that many oncologists have concluded that chemotherapy has reached a plateau in efficacy as a primary treatment modality in cancer and that a shift toward molecularly targeted agents has also had limited success in tumor growth control.[1,2] In preclinical experiments, 17-allylamino-17-demethoxygeldanamycin (17-AAG) enhanced the antitumor efficacy of PTX in human breast, lung, and ovarian xenograft models.[3−6] 17-AAG is a first-in-class inhibitor of heat shock protein 90 (Hsp90), inhibiting its function as a chaperone protein for the proper folding of oncogenic signal transduction proteins, such as Akt, ErbB2, Raf-1, and mutant EGFR.[7] Rapamycin (RAP) also enhanced the antitumor efficacy of PTX in human breast xenograft models,[8] targeting the mammalian target of rapamycin (mTOR) protein, which is centrally involved in angiogenesis, cancer cell growth, and cancer cell survival.[9] Lastly, 17-AAG sensitized the cytotoxicity of RAP against human breast cancer cells, presumably by preventing activation of Akt upon mTOR inhibition, providing a rationale for combination of 17-AAG and RAP.[10]

However, chemotherapy and molecularly targeted agents are often poorly water-soluble, necessitating toxic surfactants or cosolvents for multiple drug solubilization that add to toxicity already increased by drug combination. PTX, 17-AAG, and RAP have low water solubility (ca. 1.0 mg/L). 17-AAG required a DMSO/egg phospholipid vehicle or more recently Cremophor EL for intravenous (iv) infusion in clinical trials.[11] For clinical trials on PTX and 17-AAG, toxicity of a DMSO/egg phospholipid

Received: February 1, 2011
Accepted: June 1, 2011
Revised: May 11, 2011
Published: June 01, 2011

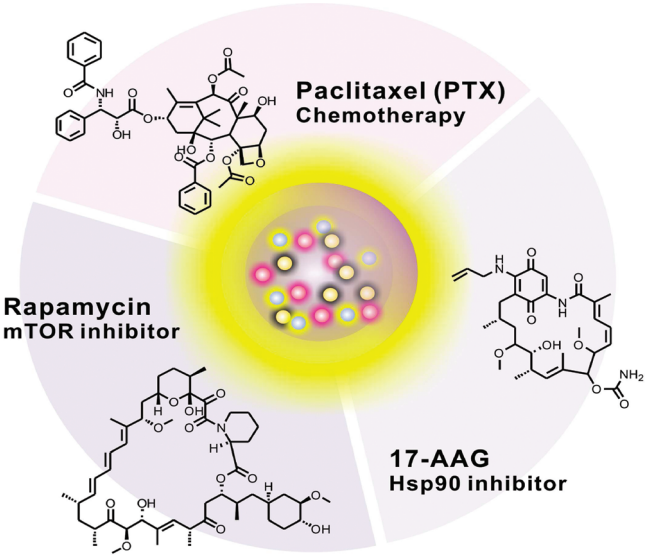

Figure 1. Schematic representation of 3-in-1 PEG-*b*-PLA micelles.

vehicle or Cremophor EL enough for the solubilization of PTX and 17-AAG is a major safety concern.[3] Rapamycin analogues (rapalogs), chemically modified for water solubility, are approved mTOR inhibitors for cancer treatment.[12] Given the odds that combination cancer treatments involving chemotherapy and molecularly targeted agents will become commonplace in preclinical drug development, pharmaceutical research on the delivery of poorly water-soluble drug combinations merits attention, aiming for multiple drug solubilization and lower toxicity than conventional iv vehicles, e.g. Cremophor EL, used in clinical trials.

Poly(ethylene glycol)-*block*-poly(D,L-lactic acid) (PEG-*b*-PLA) micelles have been widely studied in preclinical drug development for drug solubilization and drug targeting.[13] PEG-*b*-PLA micelles are attractive because of their nanoscopic dimensions, proven safety profile in humans over existing intravenous vehicles in clinical practice, and high capacity for drug solubilization.[14] Hydrophobic interaction between the cores of PEG-*b*-PLA micelles and poorly water-soluble drugs is the primary driving force for drug solubilization. A PEG-*b*-PLA micelle for PTX is approved in Korea (Genexol-PM) for cancer treatment and is in phase II clinical trials in the USA as a safer alternative to Cremophor EL and ethanol in Taxol.[15,16] Clinical studies have confirmed the safety of Genexol-PM over Taxol, higher maximum tolerated dose (MTD) of PTX, an apparent linear pharmacokinetic profile, and superior antitumor responses.[15,16]

PEG-*b*-PLA micelles may act as a 3-in-1 nanocontainer for multiple poorly water-soluble drugs, thereby providing a novel and simple approach for combination cancer treatment, involving chemotherapy and molecularly targeted agents. 3-in-1 PEG-*b*-PLA micelles offer a unique nanotechnology platform for combination cancer therapy that fulfills major drug delivery requirements for poorly water-soluble chemotherapy and molecular targeted agents: simplicity of scale-up, sterile filtration, safety, and solubilization, aiming for synergy in cancer drug development. The goal of our research is to explore the feasibility of 3-in-1 PEG-*b*-PLA micelles for multiple drug delivery: PTX, 17-AAG, and RAP (Figure 1). We hypothesized that PTX, 17-AAG, and RAP will exert synergistic anticancer activity, and that 3-in-1 PEG-*b*-PLA micelles will act as a safe nanocontainer for iv infusion of a 3-drug cocktail in combination cancer treatment.

2. MATERIALS AND METHODS

2.1. Materials. PEG-*b*-PLA (M_n of PEG = 4200 g/mol and M_n of PLA = 1900 g/mol, PDI = 1.05) was purchased from Advanced Polymer Materials Inc. (Montreal, CAN). PTX, 17-AAG, and RAP were purchased from LC Laboratories (Woburn, MA). MCF-7 human breast cancer cells were obtained from the Small Molecule Screening Center, University of Wisconsin (Madison, WI). 4T1 murine breast cancer cells were purchased from American Type Culture Collection (Manassas, VA). Dulbecco's modified Eagle's medium (DMEM), RPMI1640 with L-glutamine medium, penicillin−streptomycin liquid (100X), fetal bovine serum certified (FBS), and 0.25% trypsin−EDTA were purchased from Invitrogen (Carlsbad, CA). Cell Titer Blue cell viability assay kit was obtained from Promega Inc. (Madison, WI). All other reagents were obtained from Fisher Scientific Inc. (Fairlawn, NJ) and were of analytical grade.

2.2. Methods. *2.2.1. Preparation of 3-in-1 PEG-b-PLA Micelles.* The procedure used to prepare 3-in-1 PEG-*b*-PLA micelles was described previously.[17] Briefly, 15.0 mg of PEG-*b*-PLA, 2.0 mg of PTX, 2.0 mg of 17-AAG, and 1.5 mg of RAP were dissolved in 0.50 mL of acetonitrile and added to a 5.0 mL round-bottom flask. Acetonitrile was removed by reduced pressure using rotary evaporator at 60 °C, and polymer film was rehydrated with 0.50 mL of double-distilled H_2O (DDH_2O). This aqueous solution containing 3-in-1 PEG-*b*-PLA micelles carrying PTX, 17-AAG, and RAP was centrifuged and filtered (0.45 μm). PEG-*b*-PLA micelles carrying one or two drugs were prepared in the same way.

2.2.2. Reverse Phase HPLC (RP-HPLC) analysis of PTX, 17-AAG, and RAP. The level of drug loading in PEG-*b*-PLA micelles was quantified with a Prominence HPLC system (Shimadzu, JP), which consists of a LC-20 AT pump, a SIL-20AC HT autosampler, a CTO-20AC column oven and a SPD-M20A diode array detector. For the chromatographic separation of PTX, 17-AAG, and RAP, a Zorbax SB-C8 Rapid Resolution cartridge (4.6 × 75 mm, 3.5 μm, Agilent) was used, and the column oven was kept at 40 °C. The elution of PTX, 17-AAG, and RAP was carried out in an isocratic mode with mobile phase consisting of 55% acetonitrile and 45% water, containing 0.1% phosphoric acid and 1% methanol. The flow rate and injection volume were 1.0 mL/min and 10 μL, respectively. PTX, 17-AAG, and RAP were monitored at 227, 333, and 279 nm, respectively. The retention time of PTX, 17-AAG, and RAP was 2.8, 3.3, and 8.6 min, respectively. All samples were injected in triplicate, and the peak area from each injection was reproducible with high resolution for accurate drug quantitation. To determine the drug content of PEG-*b*-PLA micelles, aqueous solutions of PEG-*b*-PLA micelles carrying a single drug or multiple drugs were freeze-dried for 2 days using a FreeZone 4.5 system (Labconco Corp., U.S.). The freeze-dried sample was weighed, and the amounts of drug(s) in the sample was/were quantified by RP-HPLC. The amount of polymer was estimated by subtracting the amount of drug from the total mass. Percent drug loading was defined as the ratio of weight of drug(s) to weight of polymer.

2.2.3. Dynamic Light Scattering (DLS) Analysis. The dimensions of PEG-*b*-PLA micelles were evaluated by a ZETASIZER Nano-ZS (Malvern Instruments Inc., U.K.). A He−Ne laser (4 mW, 633 nm) was used as light source with a configuration of

173 ° to collect the scattered light. Prior to measuring particle size, PEG-*b*-PLA micelle solutions were diluted 20 times with DDH_2O, resulting in the level of PEG-*b*-PLA at 1.5 mg/mL (above the critical micelle concentration for the polymer). Samples were pre-equilibrated at 25 °C for 2 min then kept at 25 °C throughout the measurements. Correlation functions were obtained from the scattered light, which was then curve-fitted by the cumulant method to estimate particle size and polydispersity index (PDI). The Stokes−Einstein equation was used for the calculation of hydrodynamic diameters of PEG-*b*-PLA micelles. All measurements were obtained in triplicate, and the average volume-weighted hydrodynamic diameters with standard deviation were reported.

2.2.4. In Vitro Drug Release Experiments. PEG-*b*-PLA micelles carrying PTX, 17-AAG, RAP, or their combinations were diluted with DDH_2O, yielding approximately 100 μg/mL of each drug. Diluted micelle solutions were loaded into the dialysis cassettes at a MWCO = 20,000 g/mol (Pierce, U.S.). Four dialysis cassettes were placed in 2 L of phosphate buffer saline (pH 7.4) and maintained at 37 °C with slow stirring. The sampling time points were 0, 0.5, 2, 4, 6, 9, 12, and 24 h. At each time point, 100 μL of sample was withdrawn from dialysis cassettes and replaced with an equal volume of fresh buffer. The external medium was changed at 2, 6, and 12 h to maintain the sink conditions for polymer and drug(s). Drug concentration(s) in each sample were determined by RP-HPLC analysis. The obtained drug release profiles were curve-fit using GraphPad Prism software (Version 5.0, U.S.), calculating apparent first-order release kinetic parameters as previously described.[17]

2.2.5. In Vitro Cytotoxicity Experiments. MCF-7 and 4T1 cells were cultured in DMEM and RPMI1640 medium, respectively, supplemented with 10% FBS, 100 IU/mL penicillin, 100 μg/mL streptomycin, and 2 mM L-glutamine. The cells were maintained at 37 °C and 5% CO_2 atmosphere for the duration of experiments. Exponentially growing cancer cells were plated into a 96-well plate at a seeding density of 3000−5000 cells per well and incubated for 24 h. PTX, 17-AAG, or RAP in DMSO or in PEG-*b*-PLA micelles was added at final concentrations of 0.1, 1, 10, 100, and 1000 nM in the wells. The final level of DMSO in the culture plate wells was <0.1% after dilution with cell culture medium. MCF-7 and 4T1 breast cancer cells were incubated for 72 h, and cell viability was determined using a Cell Titer Blue assay (Promega, U.S.) with a SpectraMax M2 plate reader (Molecular Device, U.S.) (excitation at 560 and emission at 590 nm). The half maximal inhibitory drug concentration (IC_{50}) was determined by the median effect equation using CompuSyn software (Version 1.0, ComboSyn Inc., U.S.):

$$f_a = \frac{1}{\left[1 + \left(\frac{IC_{50}}{D}\right)^m\right]}$$

In the median effect equation, f_a is the fraction of affected cells; D is drug concentration; and m is the Hill slope or kinetic order. IC_{50} values for PTX, 17-AAG, RAP, and combinations were determined from 3 independent growth inhibition curves and represented as a mean ± standard deviation.

2.2.6. Combination Index (CI) Analysis. CI analysis based on Chou and Talalay method was performed using CompuSyn software (Version 1.0, ComboSyn Inc., U.S.) for PTX, 17-AAG, and RAP combinations, determining synergistic, additive, or antagonistic cytotoxic effects against MCF-7 or 4T1 breast cancer cells.[18] Briefly, f_a was determined as a function of D by the median-effect equation, varying doses from 5% of affected cells (IC_5) to 97% of affected cells (IC_{97}). CI values at each f_a for 2-drug combinations were calculated using the following equation:

$$CI = \frac{(D)_1}{(D_x)_1} + \frac{(D)_2}{(D_x)_2}$$

$(D_x)_1$ and $(D_x)_2$ represent the IC_x value of drug 1 alone and drug 2 alone, respectively. $(D)_1$ and $(D)_2$ represent the concentration of drug 1 and drug 2 at the IC_x value (x% growth inhibition). For the 3 drug combination, the following equation was used by simply adding the third term:

$$CI = \frac{(D)_1}{(D_x)_1} + \frac{(D)_2}{(D_x)_2} + \frac{(D)_3}{(D_x)_3}$$

Values of CI > 1 represent antagonism, CI = 1 represent additive and CI < 1 represent synergism. At constant drug combination ratios, f_a versus CI plots for 2- and 3-drug combinations were obtained with GraphPad prism software (Version 5.0, U.S.).

2.2.7. Acute Toxicity Experiments. All animal studies were conducted under the protocol approved by Institutional Animal Care and Use Committee (IACUC) in University of Wisconsin—Madison, and all experiments were carried out according to the NIH guide for the Care and Use of Laboratory Animals. Six to eight week old FVB female albino mice (FVB/NCrl) were purchased from Charles River Laboratories (Wilmington, MA, U.S.) and housed in ventilated cages with free water and food. Seven groups of mice (n = 3−4 per group) were used for the evaluation of acute toxicity. PEG-*b*-PLA micelles carrying PTX, 17-AAG, RAP, or their combinations were prepared freshly, reconstituted with 0.9% NaCl solution and sterilized by 0.22 μm filter. Drug concentration(s) were confirmed by RP-HPLC analysis. PEG-*b*-PLA micelles carrying PTX were injected through the tail vein at 60 mg/kg of PTX at days 0, 4, and 8. 17-AAG was dosed at 60 mg/kg, and RAP was dosed at 30 mg/kg. For 2- and 3-drug combinations, PTX, 17-AAG, and RAP were injected at identical doses. Taxol was injected at 12 mg/kg to monitor acute toxicity effects of Cremophor EL and ethanol. Acute toxicity was defined as >15% body weight loss, signs of discomfort, abnormal behavior, or death of animals.[19] Body weight changes were normalized by dividing the initial body weight of each animal and measured over 12 days; results were represented as a mean ± standard error of mean.

2.2.8. Statistical Analysis. Student's *t*-test at a 0.05% level was performed to determine the statistical significance of data.

3. RESULTS

3.1. Multiple Drug Solubilization by PEG-*b*-PLA Micelles. 3-in-1 PEG-*b*-PLA micelles had a remarkable capacity of PTX, 17-AAG, and RAP, resulting in multiple drug solubilization at 9.3 mg/mL in water and high percent drug loading at 40.4 ± 1.2% (Figure 2 and Table 1). The individual water solubility of PTX, 17-AAG, and RAP achieved by 3-in-1 PEG-*b*-PLA micelles was 3.36 ± 0.46, 3.86 ± 0.46, and 2.09 ± 0.11 mg/mL, respectively. Thus, the water solubility of PTX, 17-AAG, and RAP was increased by 10^4-, 700-, and 80-fold, respectively (intrinsic water solubility of PTX, 17-AAG, and RAP is 0.41, 50, and 2.6 μg/mL, respectively).[20−22] Similarly, 2-in-1 PEG-*b*-PLA micelles were also effective in multiple drug solubilization of

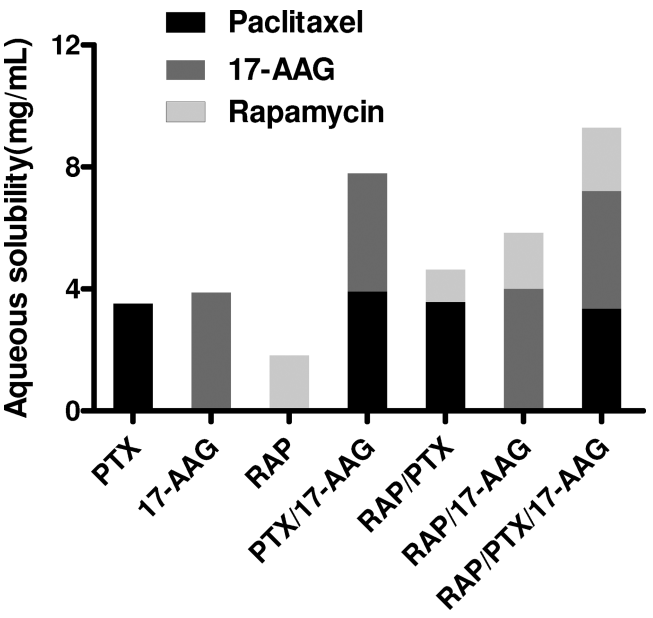

Figure 2. Aqueous solubility of PTX, 17-AAG, and RAP as singly loaded, 2-in-1, and 3-in-1 PEG-*b*-PLA micelles (n = 3, mean).

Table 1. Drug Solubilization Results for PEG-*b*-PLA Micelles (n = 3, Mean ± SD)

drug(s)	solubility (mg/mL)	drug loading (%)	total drug loading (%)	micelle diameter (nm)
PTX	3.54 ± 0.32*[a]	11.8 ± 1.1	11.8 ± 1.1	38.8 ± 0.6
17-AAG	3.90 ± 0.28*	13.0 ± 0.9	13.0 ± 0.9	39.3 ± 2.9
RAP	1.84 ± 0.26*	6.6 ± 1.3	6.6 ± 1.3	36.9 ± 1.3
PTX	3.92 ± 0.17	13.4 ± 0.9	25.9 ± 1.6	38.9 ± 1.1
17-AAG	3.88 ± 0.29	12.4 ± 0.8		
RAP	1.83 ± 0.25	8.0 ± 0.6	22.6 ± 1.6	39.4 ± 1.9
17-AAG	4.02 ± 0.14	14.6 ± 0.2		
RAP	1.06 ± 0.07	3.0 ± 0.2	13.3 ± 0.3	41.0 ± 1.5
PTX	3.59 ± 0.09	10.4 ± 0.1		
PTX	3.36 ± 0.46	15.5 ± 0.7	40.4 ± 1.2	43.8 ± 1.3
17-AAG	3.86 ± 0.46	16.2 ± 0.7		
RAP	2.09 ± 0.11	8.7 ± 0.4		

[a] Asterisk (*) denotes statistical difference at $p < 0.05$ compared with intrinsic solubility of each drug.

PTX and 17-AAG, RAP and 17-AAG, or PTX and RAP, resulting in percent drug loading at 25.9 ± 1.6, 22.6 ± 1.6 and 13.3 ± 0.3%, respectively (Table 1). Interestingly, results for the individual solubilization of PTX, 17-AAG, and RAP by PEG-*b*-PLA micelles were similar to the results for 3-in-1 and 2-in-1 PEG-*b*-PLA micelles even though the quantity of PEG-*b*-PLA used in drug solubilization experiments was unchanged. Thus, percent drug loading of PTX, 17-AAG, and RAP was 11.8 ± 1.1, 13.0 ± 0.9, and 6.6 ± 1.3%, respectively.

PEG-*b*-PLA micelles carrying a single drug or multiple drugs had an average volume-weighted hydrodynamic diameter at ca. 40 nm with polydispersity index <0.2 (Table 1). 3-in-1 PEG-*b*-PLA micelles were slightly larger, ca. 44 nm; this slight increase in particle size was not expected due to a large increase in drug loading, switching from a 1-drug to 3-drug nanocontainer.

We monitored the physical stability of PEG-*b*-PLA micelle solutions after 24 h at 25 °C by monitoring drug concentrations by RP-HPLC (data not shown). Major drug precipitation was only evident for PTX, resulting in retention of 16.2 ± 1.0% in solution after 24 h. Slight precipitation of rapamycin was noticed, but still 91.5 ± 0.2% remained in solution after 24 h. In contrast, 98.6 ± 2.4% of 17-AAG remained in solution after its solubilization by PEG-*b*-PLA micelles. 3-in-1 and 2-in-1 PEG-*b*-PLA micelles were remarkably stable with respect to drug precipitation with >93% retention in all cases (data not shown). For 3-in-1 PEG-*b*-PLA micelles, PTX, 17-AAG, and RAP were retained in solution at 97.9 ± 2.3, 96.7 ± 2.5, and 97.8 ± 2.1%, respectively, a noticeable difference in comparison to the result for PTX, singly incorporated into PEG-*b*-PLA micelles.

3.2. In *Vitro* Drug Release Kinetics. *In vitro* drug release profiles for PEG-*b*-PLA micelles are shown in Figure 3. For 3-in-1 PEG-*b*-PLA micelles, PTX, 17-AAG, and RAP were released simultaneously over the course of 24 h (Figure 3E). The rate of *in vitro* drug release for 3-in-1 PEG-*b*-PLA micelles increased in the order RAP, PTX, and 17-AAG; 68.0 ± 2.0, 78.1 ± 1.5, and 91.1 ± 0.5%, respectively, was released after 24 h. The release profiles for 3-in-1 PEG-*b*-PLA micelles approximated first-order release kinetics. The apparent first-order half-life ($t_{1/2}$) was calculated for RAP, PTX, and 17-AAG: 13.9, 9.2, and 2.52 h, respectively (Table 2). The goodness of fit (r^2) was 0.986−0.996. *In vitro* release profiles for RAP, PTX, and 17-AAG for PEG-*b*-PLA micelles as 2-drug combinations and single drugs were similar and again in the order RAP, PTX, and 17-AAG (Table 2). As single drug-loaded and 2-in-1 PEG-*b*-PLA micelles, $t_{1/2}$ values were slightly less than $t_{1/2}$ values for 3-in-1 PEG-*b*-PLA micelles. A complete *in vitro* release profile for PTX from PEG-*b*-PLA micelles could not be obtained due to precipitation of PTX during the drug release experiment (Figure 3A).

3.3. *In Vitro* Cytotoxicity. As shown in Figure 4, the IC_{50} value of free drug, i.e. PTX, RAP, and 17-AAG in DMSO, for MCF-7 human breast cancer cells was 24 ± 1, 43 ± 3, and 29 ± 6 nM, respectively, which correspond well to the reported literature values.[8,23−25] For 2-drug combinations, PTX and 17-AAG (5:1 molar ratio), PTX and RAP (1:1 molar ratio), and 17-AAG and RAP (1:1 molar ratio) had an IC_{50} value of 30 ± 4, 26 ± 14, and 44 ± 8 nM, respectively, showing no statistical differences in IC_{50} value compared to that of individual drugs in DMSO. In contrast, the IC_{50} value of the 3-drug combination of PTX, 17-AAG, and RAP (5:1:1 molar ratio) in DMSO for MCF-7 human breast cancer cells was 4 ± 3 nM, indicating stronger synergistic anticancer effects than 2-drug combinations.

The IC_{50} value of PTX, 17-AAG, and RAP in DMSO for 4T1 murine breast cancer cells was 5860 ± 1460, 86 ± 11, and 1460 ± 480 nM, respectively. For 2-drug combinations, PTX and 17-AAG (5:1 molar ratio), PTX and RAP (1:1 molar ratio), and 17-AAG and RAP (1:1 molar ratio) had an IC_{50} value of 51 ± 10, 1220 ± 75, and 302 ± 37 nM, respectively. In contrast, the IC_{50} value of the 3-drug combination of PTX, 17-AAG, and RAP (5:1:1 molar ratio) in DMSO for 4T1 murine breast cancer cells was 27 ± 5 nM, again indicating stronger synergistic anticancer effects than 2-drug combinations.

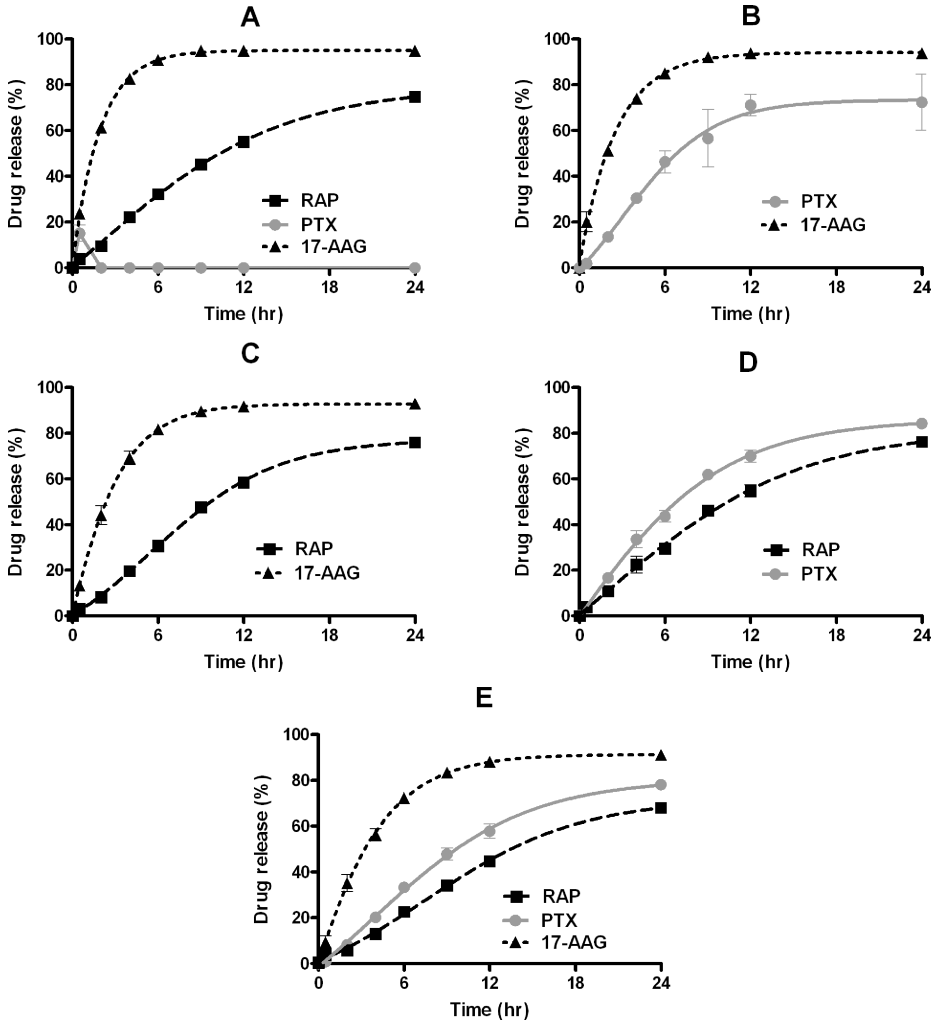

Figure 3. *In vitro* drug release profiles of (A) PTX, 17-AAG, or RAP singly loaded in PEG-*b*-PLA micelles, (B) 2-in-1 PEG-*b*-PLA micelles with PTX and 17-AAG, (C) 2-in-1 PEG-*b*-PLA micelles with RAP and 17-AAG, (D) 2-in-1 PEG-*b*-PLA micelles with PTX and RAP, and (E) 3-in-1 PEG-*b*-PLA micelles (n = 4, mean ± SD).

As shown in Figure 5, the IC_{50} value of PTX, 17-AAG, and RAP singly loaded into PEG-*b*-PLA micelles for MCF-7 human breast cancer cells was 226 ± 32, 266 ± 48, and 255 ± 37 nM, respectively; an 8- to 13-fold increase in the IC_{50} values relative to free drugs, added in DMSO. For 2-in-1 PEG-*b*-PLA micelles, PTX and 17-AAG (3.2:1 molar ratio), PTX and RAP (1:1 molar ratio), and 17-AAG and RAP (1:1 molar ratio) had an IC_{50} value of 162 ± 17, 167 ± 6, and 177 ± 3 nM, respectively. The IC_{50} value was 114 ± 10 nM for 3-in-1 PEG-*b*-PLA micelles (5:1:1 molar ratio).

The IC_{50} value of PTX, 17-AAG, and RAP singly loaded into PEG-*b*-PLA micelles for 4T1 murine breast cancer cells was 11,160 ± 4160, 118 ± 10, and >100,000 nM, respectively (Figure 5); a 2- to 10-fold increase in the IC_{50} values relative to free drugs, added in DMSO. For 2-in-1 PEG-*b*-PLA micelles, PTX and 17-AAG (4.7:1 molar ratio), PTX and RAP (1:1 molar ratio), and 17-AAG and RAP (1:1 molar ratio) had an IC_{50} value of 92 ± 19, 4010 ± 3610, and 147 ± 11 nM, respectively. The IC_{50} value was 25 ± 1 nM for 3-in-1 PEG-*b*-PLA micelles (5:1:1 molar ratio), providing a significantly lower IC_{50} value over singly loaded and 2-in-1 PEG-*b*-PLA micelles ($p < 0.05$). Collectively, our results suggest that 3-in-1 PEG-*b*-PLA micelles have superior cytotoxicity against MCF-7 human and 4T1 murine breast cancer cells.

3.4. CI Analysis. The CI values of 2-in-1 and 3-in-1 PEG-*b*-PLA micelles for MCF-7 human and 4T1 murine breast cancer cells are listed in Table 3. The CI value at IC_{50} for 2-in-1 (PTX and 17-AAG, PTX and RAP, 17-AAG and RAP), and 3-in-1 PEG-*b*-PLA micelles was 0.69 ± 0.07, 0.69 ± 0.02, 0.68 ± 0.01, and 0.49 ± 0.04, respectively, indicating synergistic cytotoxicity against MCF-7 human breast cancer cells. Similarly, the CI value at IC_{50} for 2-in-1 (PTX and 17-AAG, PTX and RAP, 17-AAG and RAP) and 3-in-1 PEG-*b*-PLA micelles was 0.14 ± 0.03, 0.19 ± 0.17, 0.62 ± 0.05, and 0.04 ± 0.001, respectively, indicating strong synergistic cytotoxicity against 4T1 murine breast cancer cells. In particular, CI values of 3-in-1 PEG-*b*-PLA micelles were the lowest for both breast cancer cell lines, indicating the strongest synergy ($p < 0.05$).

In f_a versus CI plots for 2-in-1 PEG-*b*-PLA micelles (PTX and 17-AAG, or PTX and RAP), CI values were >1.0 in the highly affected region ($f_a > 0.8$), suggesting a slightly antagonistic effect for MCF-7 human and 4T1 breast cancer cells (Figure 6). 2-in-1 PEG-*b*-PLA micelles of 17-AAG and RAP were largely synergistic at $f_a > 0.8$. Notably, the CI values of 3-in-1 PEG-*b*-PLA micelles for MCF-7 human and 4T1 murine breast cancer cells were always <1.0 over all f_a values, suggesting strong

synergistic cytotoxicity even in the highly affected region (f_a > 0.8).

3.5. Acute Toxicity Experiments. As shown in Figure 7, the iv injection of PTX, 17-AAG, and RAP singly loaded into PEG-*b*-PLA micelles at 60, 60, and 30 mg/kg, respectively, did not produce body weight loss or death after injections on days 0, 4, and 8 in 6 to 8 week old FVB female albino mice. In contrast, a toxic response such as loss of consciousness for a few minutes, flushed skin, and dyspnea for Taxol at 12 mg/kg was observed (data not shown). 2-in-1 PEG-*b*-PLA micelles carrying PTX and 17-AAG, or PTX and RAP, dosed at 60/60 or 60/30 mg/kg, respectively, had <10% weight loss upon concurrent injection and no death, suggesting a lack of overlapping toxicity. Notably, mice injected with 3-in-1 PEG-*b*-PLA micelles, dosed at 60, 60, and 30 mg/kg for PTX, 17-AAG, and RAP, respectively, had <10% of loss in body weight and no deaths over 12 days.

Table 2. *In Vitro* Release of Drug(s) for PEG-*b*-PLA Micelles (n = 4, Mean ± SD)

drug(s)	first-order rate constant (h^{-1})	$t_{1/2}$ (h)	goodness of fit (r^2)	log P^a
PTX	na[b]	na	na	3.0
17-AAG	0.525	1.32	0.999	1.3
RAP	0.081	8.52	0.990	5.8
PTX	0.138	5.01	0.938	3.0
17-AAG	0.398	1.74	0.996	1.3
RAP	0.079	8.73	0.983	5.8
17-AAG	0.385	1.80	0.999	1.3
RAP	0.069	10.05	0.991	5.8
PTX	0.116	6.00	0.993	3.0
RAP	0.050	13.93	0.986	5.8
PTX	0.075	9.20	0.984	3.0
17-AAG	0.275	2.52	0.996	1.3

[a] Calculated from XLog P ver2.0 (http://pubchem.ncbi.nlm.nih.gov/). [b] Not applicable.

4. DISCUSSION

The combination of chemotherapy and molecularly targeted agents is drawing increasing attention in preclinical and clinical cancer research in efforts seeking synergistic anticancer activity and avoidance of drug resistance. Two major requirements for evaluation in clinical trials are manageable toxicity of chemotherapy and molecularly targeted agent combinations and sufficient water solubility for iv infusion. Additive or synergistic toxicity is undesirable and may prohibit entry into clinical trials. The requirement of drug solubilization is common in preclinical drug development, mandating iv vehicles, such as Cremophor EL and cosolvents, which exacerbate the toxicity of drug combinations and mandate sequential iv infusion, owing to the risk of incompatibility and drug precipitation.[26] Thus, 2-in-1 and 3-in-1 PEG-*b*-PLA micelles may play a unique role in drug delivery as a nanocontainer for multiple poorly water-soluble anticancer agents, aiming for multiple drug solubilization with minimized toxicity.

PEG-*b*-PLA micelles dramatically increased the water solubility of PTX, 17-AAG and RAP as single drugs and 2- and 3-drug combinations (Figure 2 and Table 1). Remarkably, the content of individual drugs in 2-in-1 and 3-in-1 PEG-*b*-PLA micelles was similar to the drug content of singly loaded PEG-*b*-PLA micelles, noting that 3-in-1 PEG-*b*-PLA micelles had a 40% drug content. This increase in drug loading upon the coincorporation of one or two drugs was noticed in prior work that first established the capacity of PEG-*b*-PLA micelles for multiple drug solubilization (PTX, docetaxel, 17-AAG, and etoposide).[17] In this work, we showed that 17-AAG is not unique in its ability to produce this unusual drug solubilization behavior: RAP also pairs with PTX, resulting in 23% drug loading and a highly stable aqueous solution with ca. 96% in solution after 24 h. In contrast, drug precipitation was clearly evident for PTX after 24 h. The high drug content and physical stability of 2-in-1 and 3-in-1 PEG-*b*-PLA

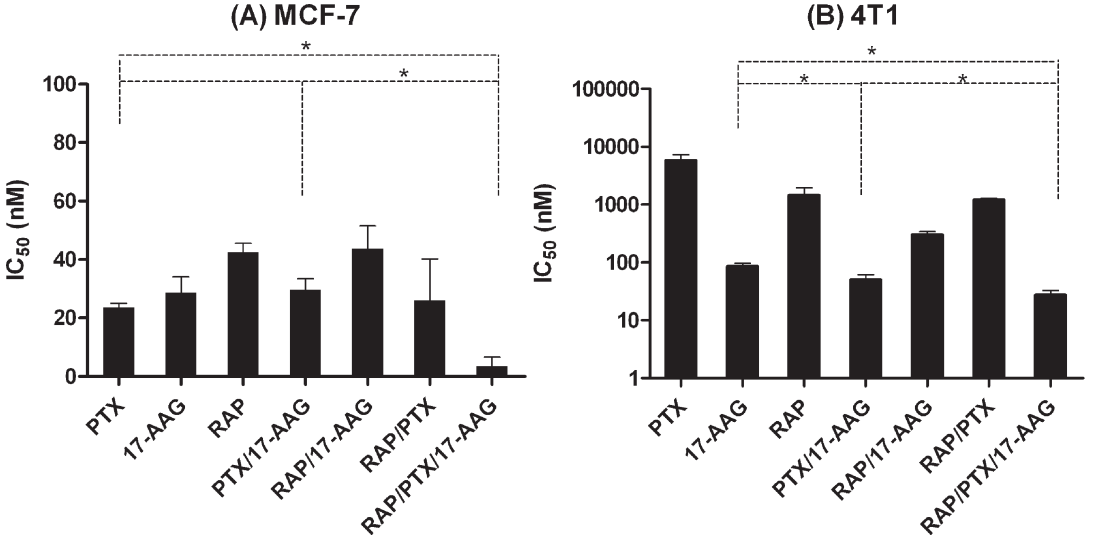

Figure 4. IC_{50} values of free drugs (dissolved in DSMO) for (A) MCF-7 human and (B) 4T1 murine breast cancer cells (n = 3, mean ± SD). Asterisk (*) denotes statistical difference at p < 0.05.

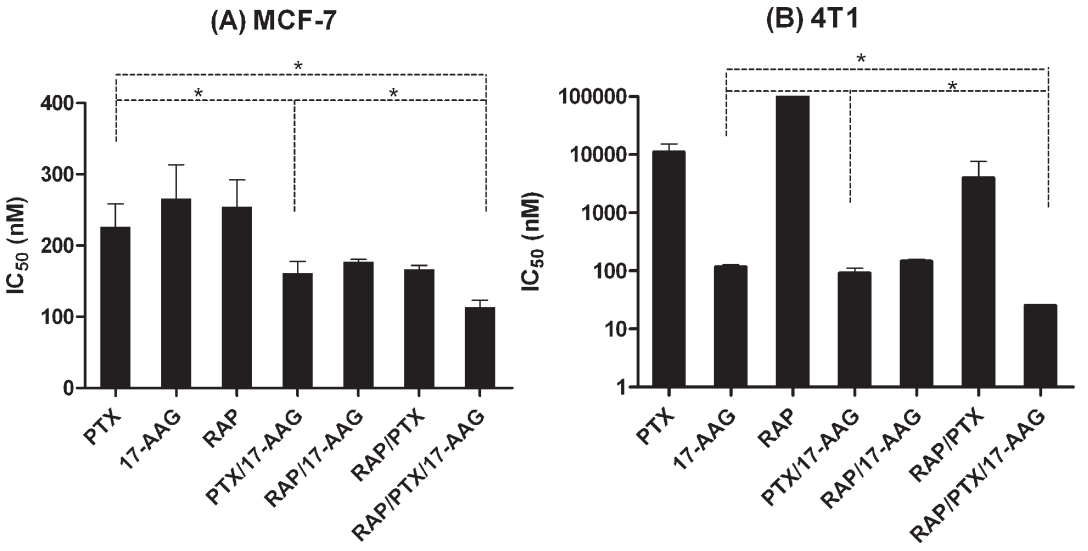

Figure 5. IC_{50} values of PTX, 17-AAG, and RAP as singly loaded, 2-in-1, and 3-in-1 PEG-*b*-PLA micelles for (A) MCF-7 human and (B) 4T1 murine breast cancer cells. Asterisk (*) denotes statistical difference at $p < 0.05$.

Table 3. CI Analysis of 2-in-1 and 3-in-1 PEG-*b*-PLA Micelles for MCF-7 Human and 4T1 Murine Breast Cancer Cells

drug(s)	molar ratio	MCF-7	4T1	drug interaction
PTX/17-AAG	3.2:1 (4.7:1)	0.69 ± 0.07	0.14 ± 0.03	synergistic
RAP/17-AAG	1:1	0.68 ± 0.01	0.62 ± 0.05	synergistic
RAP/PTX	1:1	0.69 ± 0.02	0.19 ± 0.17	synergistic
PTX/17-AAG/RAP	5:1:1	0.49 ± 0 0.04	0.04 ± 0.001	synergistic

micelles is presumably due to intermolecular interaction among drugs in the core region, but this hypothesis requires further support. Notably, the water solubility of PTX, 17-AAG and RAP as single drugs and 2- and 3-drug combinations is sufficient for experiments in human xenograft models and therapeutic applications in humans, and 2-in-1 and 3-in-1 PEG-*b*-PLA micelles are exceptional, allowing for the concurrent iv infusion of multiple drugs for cancer treatment for the first time.

3-in-1 PEG-*b*-PLA micelles simultaneously released PTX, 17-AAG, and RAP over 24 h *in vitro* (Figure 3), and it was apparent that the rates of drug release from 3-in-1 PEG-*b*-PLA micelles are slower than the rates for singly loaded and 2-in-1 PEG-*b*-PLA micelles (Table 2): the $t_{1/2}$ value for RAP, PTX, and 17-AAG for 3-in-1 PEG-*b*-PLA micelles was 13.9, 9.2, and 2.52 h, respectively, whereas the $t_{1/2}$ value was 9−10, 5−6, and 1.7−1.8 h, respectively, for 2-in-1 PEG-*b*-PLA micelles. We suspect that the lower rates of drug release for 3-in-1 PEG-*b*-PLA micelles are a reflection of intermolecular interaction among drugs in the core region, noticed in drug solubilization experiments. The $t_{1/2}$ values for RAP, PTX, and 17-AAG correlated well with logarithm of oil−water partition coefficient (log *P*) as shown in Table 2, confirming the importance of lipophilicity in the *in vitro* kinetics of drug release for PEG-*b*-PLA micelles, but not for drug solubilization.

After the iv injection of 3-in-1 PEG-*b*-PLA micelles, it is tempting to speculate that the rank order of drug release will remain the same, drug release will be complete within 24 h, and the likelihood that 3-in-1 PEG-*b*-PLA micelles stay associated

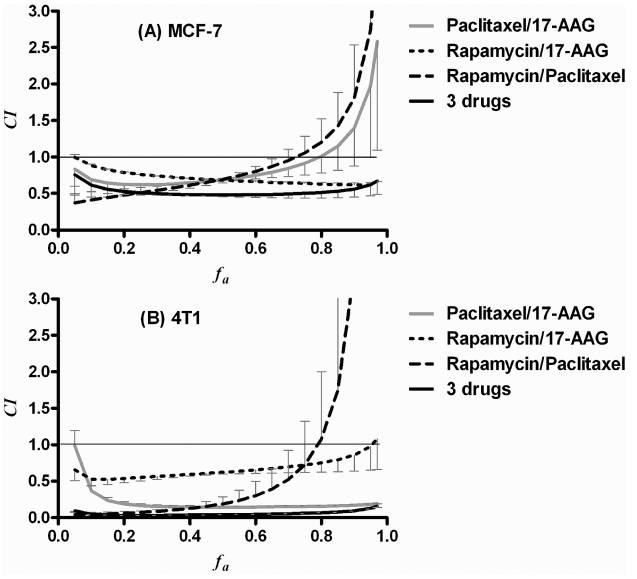

Figure 6. f_a−CI plots of 2-in-1, and 3-in-1 PEG-*b*-PLA micelles for (A) MCF-7 human and (B) 4T1 murine breast cancer cells ($n = 3$, mean ± SD).

with drug and influence its pharmacokinetics is greatest for RAP and PTX and least for 17-AAG. Thus, PEG-*b*-PLA micelles will favor the preferential accumulation of RAP and PTX at solid tumors via the enhanced permeability and retention (EPR) effect over 17-AAG. However, 17-AAG and Hsp90 inhibitors in general accumulate favorably at solid tumors, presumably due to an overexpression of Hsp90 (ca. 4−6% of all proteins).[27] Thus, we raise the feasibility of a simultaneous accumulation of PTX, 17-AAG, and RAP at solid tumors for synergistic cancer cell killing after the iv injection of 3-in-1 PEG-*b*-PLA micelles.

In cell culture experiments, 3-in-1 PEG-*b*-PLA micelles had the highest cytotoxicity (lowest IC_{50} values) against MCF-7 human and 4T1 murine breast cancer cells (Figure 5). CI analysis indicated that 3-in-1 PEG-*b*-PLA micelles have the highest synergy for both breast cancer cell lines. Furthermore, f_a versus

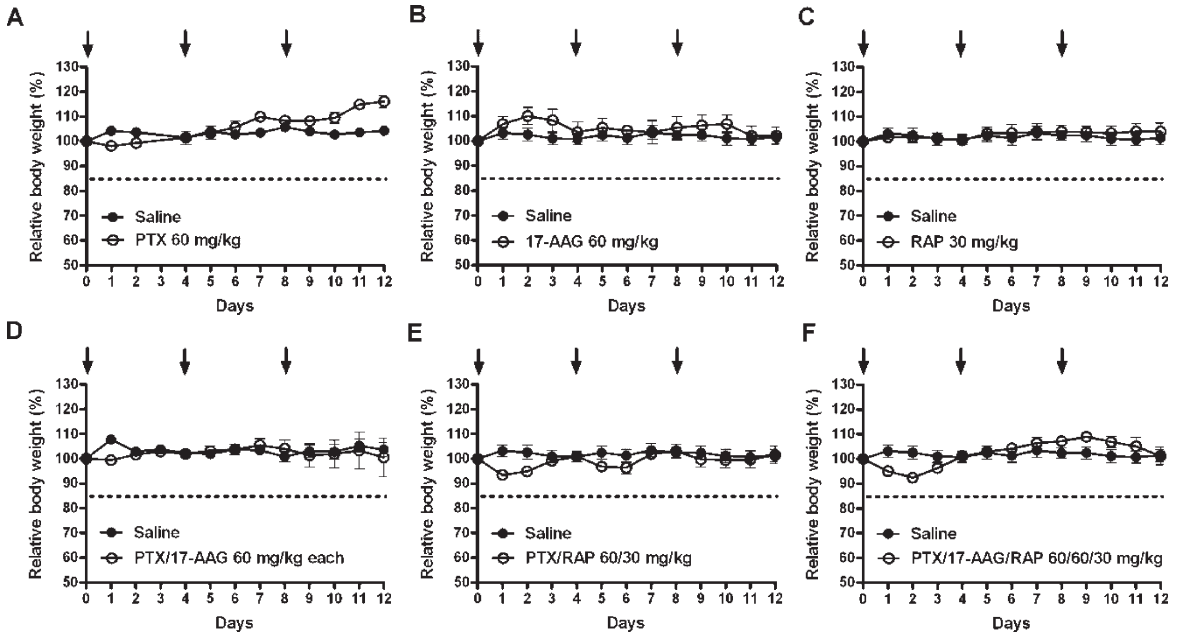

Figure 7. Relative body weight of mice over time after iv injection of PTX, 17-AAG, and RAP as singly loaded, 2-in-1, and 3-in-1 PEG-*b*-PLA micelles on days 0, 4, and 8. (A) PTX at 60 mg/kg, (B) 17-AAG at 60 mg/kg, (C) RAP at 30 mg/kg, (D) PTX and 17-AAG at 60 and 60 mg/kg, (E) PTX and RAP at 60 and 30 mg/kg, and (F) PTX, 17-AAG and RAP at 60, 60, and 30 mg/kg (n = 3−4/treatment, mean ± SEM).

CI plots of 3-in-1 PEG-*b*-PLA micelles showed synergistic cytotoxicity over all f_a (fraction affected), in contrast to 2-in-1 PEG-*b*-PLA micelles (Figure 6), suggesting synergy even at high effect levels, which are most relevant to cancer therapy.[18] It is noted that results for free drugs and their combinations were consistent with the results for drugs in PEG-*b*-PLA micelles (Figure 5) and that the generally higher IC_{50} values in the latter case can be ascribed to the association of drug(s) and PEG-*b*-PLA micelles in cell culture.

4T1 murine breast cancer cells (a spontaneous mammary carcinoma cell line) were resistant toward PTX (Figure 5). However, 3-in-1 PEG-*b*-PLA micelles were highly cytotoxic toward 4T1 murine breast and MCF-7 human breast cancer cells, raising the feasibility of a new treatment for metastatic breast cancer. We hypothesize that 17-AAG (Hsp90 inhibitor) and RAP (mTOR inhibitor) enhance the cytotoxicity of PTX (mitosis inhibitor) against breast cancer cells by acting on two major cancer survival pathways: PI3K/Akt/mTOR and Ras/Raf/MEK/ERK pathways; biochemical tests are ongoing to assess this hypothesis, along with cell culture tests and CI analysis that will definitively define drug ratios for PTX, 17-AAG, and RAP that are synergistic, additive, or even perhaps antagonistic.

Besides the unusually high capacity of PEG-*b*-PLA micelles for PTX, 17-AAG, and RAP in terms of drug solubilization and nM potency against MCF-7 and 4T1 breast cancer cells, the low acute toxicity of 3-in-1 PEG-*b*-PLA micelles was exceptional (Figure 7). Remarkably, mice received PTX, 17-AAG, and RAP without a dose reduction for PTX (60 mg/kg). The MTD for Genexol-PM (PTX singly loaded into PEG-*b*-PLA micelles) was defined at 60 mg/kg in nude mice, whereas the MTD for Taxol was 20 mg/kg.[28] Clinically, replacement of Cremophor EL with PEG-*b*-PLA enabled a doubling of PTX dose and greater antitumor efficacy.[29] 3-in-1 PEG-*b*-PLA micelles now allow for the added injection of 17-AAG and RAP at 60 and 30 mg/kg with minimal weight loss in mice and no deaths, seeking synergy. In contrast, intraperitoneal injections of paclitaxel and 17-AAG in a DMSO/egg phospholipid vehicle caused two early deaths of mice.[3] For 3-in-1 and 2-in-1 PEG-*b*-PLA micelles, acute toxicity was surprisingly low even though peak plasma concentrations of PTX, 17-AAG, and RAP will occur at similar times, owing to their simultaneous iv injection. The dose-limiting toxicity of PTX is neutropenia and neurotoxicity.[30] RAP causes dose-limiting mucosititis, asthenia, and thrombocytopenia.[31] 17-AAG causes dose-limiting hepatotoxicity, although its effects may be secondary to the DMSO/egg phospholipid vehicle.[32] Thus, the toxicities of PTX, 17-AAG, and RAP appear to be nonadditive as 3-in-1 PEG-*b*-PLA micelles, although their preclinical toxicity profile needs to be further defined. Importantly, drug ratios of 3-in-1 PEG-*b*-PLA micelles may be adjusted in the case of untoward toxicity and certainly sequential drug injections may also be an alternative strategy. Given this flexibility in the delivery of PTX, 17-AAG, and RAP along with nM potency against MCF-7 and 4T1 breast cancer cells, 3-in-1 PEG-*b*-PLA micelles merit evaluation in human breast xenograft models.

■ ASSOCIATED CONTENT

Supporting Information. Particle size distribution of singly loaded, 2-in-1, and 3-in-1 PEG-*b*-PLA micelles by DLS and *in vitro* cytotoxicity experiments for determining the drug ratio of PTX/17-AAG and PTX/17-AAG/RAP in MCF-7 breast cancer cell line. This material is available free of charge via the Internet at http://pubs.acs.org.

■ AUTHOR INFORMATION

Corresponding Author

*School of Pharmacy, University of Wisconsin, 777 Highland Ave., Madison, WI 53705-2222. Phone: +1-608-265-5183. Fax: +1-608-262-5345. E-mail: gskwon@pharmacy.wisc.edu.

■ ACKNOWLEDGMENT

We thank Noel Peters at Small Molecule Screening Facility (SMSF) in the University of Wisconsin for the kind gift of MCF-7 cells. We thank Zhisheng Jiang for assistance with the animal studies.

■ REFERENCES

(1) Bagnyukova, T.; Serebriiskii, I. G.; Zhou, Y.; Hopper-Borge, E. A.; Golemis, E. A.; Astsaturov, I. Chemotherapy and signaling: How can targeted therapies supercharge cytotoxic agents? *Cancer Biol Ther.* **2010**, *10* (9), 839–53.

(2) LoPiccolo, J.; Blumenthal, G. M.; Bernstein, W. B.; Dennis, P. A. Targeting the PI3K/Akt/mTOR pathway: effective combinations and clinical considerations. *Drug Resist. Updates* **2008**, *11* (1−2), 32–50.

(3) Solit, D. B.; Basso, A. D.; Olshen, A. B.; Scher, H. I.; Rosen, N. Inhibition of heat shock protein 90 function down-regulates Akt kinase and sensitizes tumors to Taxol. *Cancer Res.* **2003**, *63* (9), 2139–44.

(4) Munster, P. N.; Basso, A.; Solit, D.; Norton, L.; Rosen, N. Modulation of Hsp90 function by ansamycins sensitizes breast cancer cells to chemotherapy-induced apoptosis in an RB- and schedule-dependent manner. See: E. A. Sausville, Combining cytotoxics and 17-allylamino, 17-demethoxygeldanamycin: sequence and tumor biology matters, Clin. *Cancer Res.* **2001**, *7*, 2155–8. *Clin. Cancer Res.* **2001**, *7* (8), 2228–36.

(5) Nguyen, D. M.; Lorang, D.; Chen, G. A.; Stewart, J. H. t.; Tabibi, E.; Schrump, D. S. Enhancement of paclitaxel-mediated cytotoxicity in lung cancer cells by 17-allylamino geldanamycin: in vitro and in vivo analysis. *Ann. Thorac. Surg.* **2001**, *72*, (2), 371−8; discussion 378−9.

(6) Sain, N.; Krishnan, B.; Ormerod, M. G.; De Rienzo, A.; Liu, W. M.; Kaye, S. B.; Workman, P.; Jackman, A. L. Potentiation of paclitaxel activity by the HSP90 inhibitor 17-allylamino-17-demethoxygeldanamycin in human ovarian carcinoma cell lines with high levels of activated AKT. *Mol. Cancer Ther.* **2006**, *5* (5), 1197–208.

(7) Solit, D. B.; Chiosis, G. Development and application of Hsp90 inhibitors. *Drug Discovery Today* **2008**, *13* (1−2), 38–43.

(8) Mondesire, W. H.; Jian, W.; Zhang, H.; Ensor, J.; Hung, M. C.; Mills, G. B.; Meric-Bernstam, F. Targeting mammalian target of rapamycin synergistically enhances chemotherapy-induced cytotoxicity in breast cancer cells. *Clin. Cancer Res.* **2004**, *10* (20), 7031–42.

(9) Dancey, J. E. Therapeutic targets: MTOR and related pathways. *Cancer Biol. Ther.* **2006**, *5* (9), 1065–73.

(10) Roforth, M. M.; Tan, C. Combination of rapamycin and 17-allylamino-17-demethoxygeldanamycin abrogates Akt activation and potentiates mTOR blockade in breast cancer cells. *Anticancer Drugs* **2008**, *19* (7), 681–8.

(11) Bagatell, R.; Gore, L.; Egorin, M. J.; Ho, R.; Heller, G.; Boucher, N.; Zuhowski, E. G.; Whitlock, J. A.; Hunger, S. P.; Narendran, A.; Katzenstein, H. M.; Arceci, R. J.; Boklan, J.; Herzog, C. E.; Whitesell, L.; Ivy, S. P.; Trippett, T. M. Phase I pharmacokinetic and pharmacodynamic study of 17-N-allylamino-17-demethoxygeldanamycin in pediatric patients with recurrent or refractory solid tumors: a pediatric oncology experimental therapeutics investigators consortium study. *Clin. Cancer Res.* **2007**, *13* (6), 1783–8.

(12) Wang, X.; Sun, S. Y. Enhancing mTOR-targeted cancer therapy. *Expert Opin. Ther. Targets* **2009**, *13* (10), 1193–203.

(13) Aliabadi, H. M.; Lavasanifar, A. Polymeric micelles for drug delivery. *Expert Opin. Drug Delivery* **2006**, *3* (1), 139–62.

(14) Kwon, G. S. Editorial for theme section on polymeric micelles for drug delivery. *Pharm. Res.* **2008**, *25* (9), 2053–5.

(15) Kim, D. W.; Kim, S. Y.; Kim, H. K.; Kim, S. W.; Shin, S. W.; Kim, J. S.; Park, K.; Lee, M. Y.; Heo, D. S. Multicenter phase II trial of Genexol-PM, a novel Cremophor-free, polymeric micelle formulation of paclitaxel, with cisplatin in patients with advanced non-small-cell lung cancer. *Ann. Oncol.* **2007**, *18* (12), 2009–14.

(16) Lee, K. S.; Chung, H. C.; Im, S. A.; Park, Y. H.; Kim, C. S.; Kim, S. B.; Rha, S. Y.; Lee, M. Y.; Ro, J. Multicenter phase II trial of Genexol-PM, a Cremophor-free, polymeric micelle formulation of paclitaxel, in patients with metastatic breast cancer. *Breast Cancer Res. Treat.* **2008**, *108* (2), 241–50.

(17) Shin, H. C.; Alani, A. W.; Rao, D. A.; Rockich, N. C.; Kwon, G. S. Multi-drug loaded polymeric micelles for simultaneous delivery of poorly soluble anticancer drugs. *J. Controlled Release* **2009**, *140* (3), 294–300.

(18) Chou, T. C. Theoretical basis, experimental design, and computerized simulation of synergism and antagonism in drug combination studies. *Pharmacol. Rev.* **2006**, *58* (3), 621–81.

(19) Freireich, E. J.; Gehan, E. A.; Rall, D. P.; Schmidt, L. H.; Skipper, H. E. Quantitative comparison of toxicity of anticancer agents in mouse, rat, hamster, dog, monkey, and man. *Cancer Chemother. Rep.* **1966**, *50* (4), 219–44.

(20) Liggins, R. T.; Hunter, W. L.; Burt, H. M. Solid-state characterization of paclitaxel. *J. Pharm. Sci.* **1997**, *86* (12), 1458–63.

(21) Simamora, P.; Alvarez, J. M.; Yalkowsky, S. H. Solubilization of rapamycin. *Int. J. Pharm.* **2001**, *213* (1−2), 25–9.

(22) Sydor, J. R.; Normant, E.; Pien, C. S.; Porter, J. R.; Ge, J.; Grenier, L.; Pak, R. H.; Ali, J. A.; Dembski, M. S.; Hudak, J.; Patterson, J.; Penders, C.; Pink, M.; Read, M. A.; Sang, J.; Woodward, C.; Zhang, Y.; Grayzel, D. S.; Wright, J.; Barrett, J. A.; Palombella, V. J.; Adams, J.; Tong, J. K. Development of 17-allylamino-17-demethoxygeldanamycin hydroquinone hydrochloride (IPI-504), an anti-cancer agent directed against Hsp90. *Proc. Natl. Acad. Sci. U.S.A.* **2006**, *103* (46), 17408–13.

(23) Merlin, J. L.; Barberi-Heyob, M.; Bachmann, N. In vitro comparative evaluation of trastuzumab (Herceptin) combined with paclitaxel (Taxol) or docetaxel (Taxotere) in HER2-expressing human breast cancer cell lines. *Ann. Oncol.* **2002**, *13* (11), 1743–8.

(24) Xiong, M. P.; Yanez, J. A.; Kwon, G. S.; Davies, N. M.; Forrest, M. L. A cremophor-free formulation for tanespimycin (17-AAG) using PEO-b-PDLLA micelles: characterization and pharmacokinetics in rats. *J. Pharm. Sci.* **2009**, *98* (4), 1577–86.

(25) Robinson, B. W.; Ostruszka, L.; Im, M. M.; Shewach, D. S. Promising combination therapies with gemcitabine. *Semin. Oncol.* **2004**, *31* (2 Suppl. 5), 2–12.

(26) ten Tije, A. J.; Verweij, J.; Loos, W. J.; Sparreboom, A. Pharmacological effects of formulation vehicles: implications for cancer chemotherapy. *Clin. Pharmacokinet.* **2003**, *42* (7), 665–85.

(27) Banerji, U.; Walton, M.; Raynaud, F.; Grimshaw, R.; Kelland, L.; Valenti, M.; Judson, I.; Workman, P. Pharmacokinetic-pharmacodynamic relationships for the heat shock protein 90 molecular chaperone inhibitor 17-allylamino, 17-demethoxygeldanamycin in human ovarian cancer xenograft models. *Clin. Cancer Res.* **2005**, *11* (19 Part 1), 7023–32.

(28) Kim, S. C.; Kim, D. W.; Shim, Y. H.; Bang, J. S.; Oh, H. S.; Wan Kim, S.; Seo, M. H. In vivo evaluation of polymeric micellar paclitaxel formulation: toxicity and efficacy. *J. Controlled Release* **2001**, *72* (1−3), 191–202.

(29) Hennenfent, K. L.; Govindan, R. Novel formulations of taxanes: a review. Old wine in a new bottle? *Ann Oncol.* **2006**, *17* (5), 735–49.

(30) Marupudi, N. I.; Han, J. E.; Li, K. W.; Renard, V. M.; Tyler, B. M.; Brem, H. Paclitaxel: a review of adverse toxicities and novel delivery strategies. *Expert Opin. Drug Saf.* **2007**, *6* (5), 609–21.

(31) Raymond, E.; Alexandre, J.; Faivre, S.; Vera, K.; Materman, E.; Boni, J.; Leister, C.; Korth-Bradley, J.; Hanauske, A.; Armand, J. P. Safety and pharmacokinetics of escalated doses of weekly intravenous infusion of CCI-779, a novel mTOR inhibitor, in patients with cancer. *J. Clin. Oncol.* **2004**, *22* (12), 2336–47.

(32) Solit, D. B.; Ivy, S. P.; Kopil, C.; Sikorski, R.; Morris, M. J.; Slovin, S. F.; Kelly, W. K.; DeLaCruz, A.; Curley, T.; Heller, G.; Larson, S.; Schwartz, L.; Egorin, M. J.; Rosen, N.; Scher, H. I. Phase I trial of 17-allylamino-17-demethoxygeldanamycin in patients with advanced cancer. *Clin. Cancer Res.* **2007**, *13* (6), 1775–82.